# Cruise Report: R/V Pelican Cruise PE 04-49
Atwater Valley Electromagnetic Survey and Camera Tow

Chief Scientist: Rob. L. Evans
Woods Hole Oceanographic Institution

Captain: Craig LeBoeuf

Participants: Dan Fornari, Scientist WHOI
Mike Boyle, USGS Menlo Park
Jennifer Dougherty, USGS, Menlo Park
John Evans, USGS Woods Hole
Alan Gardner, Engineer WHOI
Lauren Gilbert, USGS Woods Hole
Marshall Swartz, Engineer WHOI

Collaborators: Deborah Hutchinson, USGS Woods Hole
Pat Hart, USGS Menlo Park
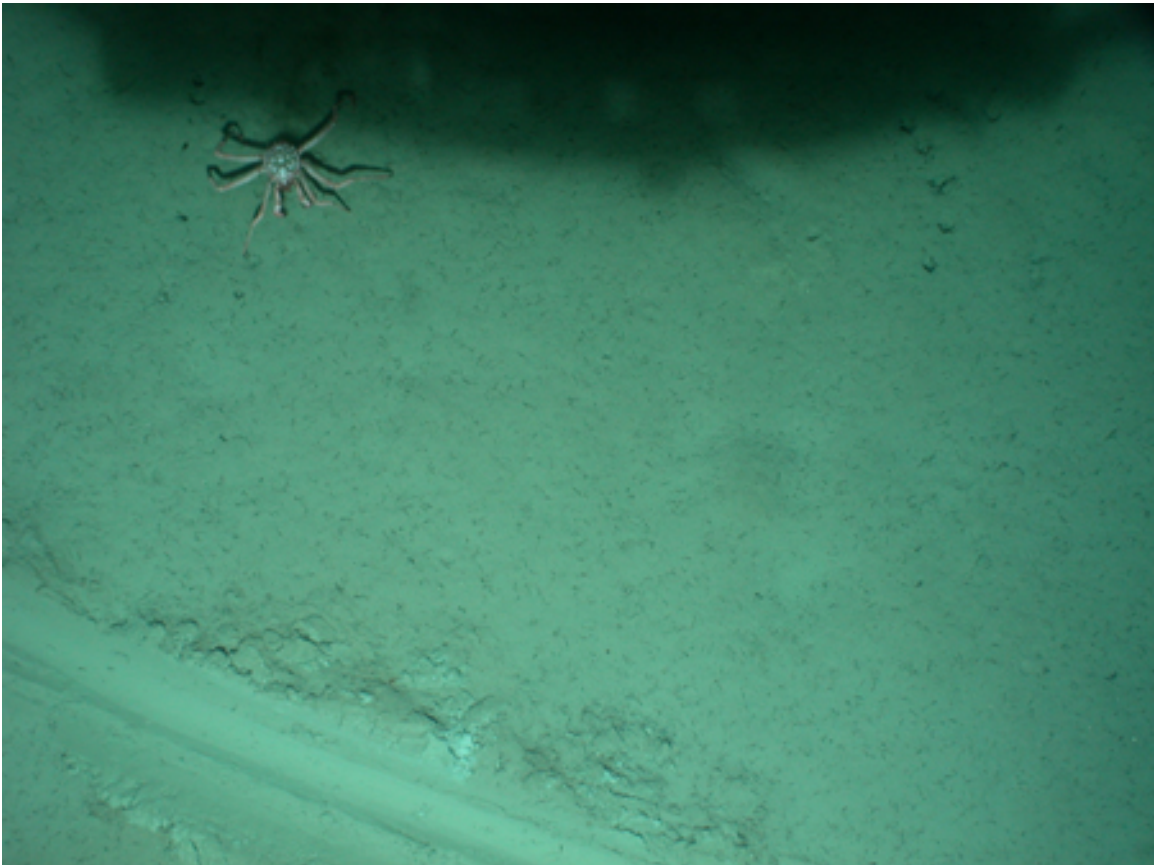
Introduction

Gas hydrate distributions within sediments on continental margins have important ramifications for the global carbon budget, for climate, for future energy resources and for slope stability and evolution (e.g., Kvenvolden, 1993). High-resolution geophysical techniques that image the shallowmost occurrences of gas-hydrate hold great potential for providing measures of the regional methane flux conditions, but large uncertainties remain about how hydrates are distributed within seafloor sediments, the importance of localized concentrations of hydrate, and the role that focused fluid flow plays in controlling these localized concentrations.

This report describes the science conducted in Atwater Valley, Gulf of Mexico from June 20th-24th. The aim of the cruise was to complete a series of seafloor electromagnetic survey lines and near-bottom camera tows across a region of seafloor thought to contain gas-hydrate bearing mounds. The electromagnetic survey was a proof of concept, collecting sample lines in well surveyed areas. Our results will be used to develop a strategy for obtaining maps of shallow hydrate distributions which can be used to test flux based models of hydrate formation and to examine links between shallow hydrates and faults and other conduits that channel methane and fluids to the seafloor.

Acknowledgements

Objectives

The primary objective during the cruise was to conduct a pilot study, testing the ability of a towed electromagnetic (EM) system to delineate regions of shallow gas hydrate and to determine the sub-seafloor structure of hydrate bearing mounds in the Gulf of Mexico (GOM). This survey consisted of running lines in an area that had been previously imaged using high resolution seismic reflection profiling (Hutchinson and Hart, 2004)

and that has been chosen as a target for drilling in a joint industry and academic research program (JIP).

The need for this new EM approach arises from the inability of existing sampling and geophysical methods to readily provide maps of shallow hydrate concentrations. Knowledge of the extent of such deposits is important for several reasons. First, these hydrates represent a readily available source of methane to the deep ocean, potentially important both from a resource and a climatologic viewpoint. Second, the presence of hydrate in the shallow seafloor is thought to be caused by high fluxes of methane from depth, carried by fluids through faults and vents. Finally, mapping the internal structures of these features provides information for understanding deeper fluid flow and its effects on seafloor stability.

The towed EM system used measures electrical resistivity profiles to depths of around 20 m below the seafloor. The system is pulled across the seafloor and with the data collected we will be able to create a map of physical properties. The presence of gas hydrate is expected to increase the seafloor resistivity by an easily measurable and identifiable amount. Gas hydrates are solids, composed of cages of water molecules that trap molecules of gas (Sloan, 1998). To first order, the presence of gas hydrate within the sediment framework will act as an electrical insulator, increasing resistivity by several orders of magnitude (e.g., Pearson et al., 1986). However, the degree to which the bulk resistivity will be increased by the solid hydrate phase depends on the hydrate concentration and how the hydrate is distributed between grains. In many instances we expect to survey fault controlled and massive hydrate bodies. It is reasonable to expect that such features will constitute significant resistivity anomalies, easily measurable with the towed system. Additional increases in resistivity around hydrate mounds and hydrate filled cracks and faults might also occur and might be due to carbonate cementation, pore water freshening and free gas (see Evans et al., 1999).

It is known that many of the mounds in the Gulf of Mexico have significantly elevated heat fluxes. Elevated temperatures, caused by regions of upwelling hot fluids in the subbottom, would cause a decrease in resistivity. Increases in pore fluid chlorinity would also cause a decrease in bulk resistivity. Thus, we expect there to be competing signals which will have opposite effects on the data that we measure, but which will allow us to constrain the thermal and lithologic structure of the mounds and surroundings.

In addition to EM profiling, we also carried out a series of near-seafloor camera tows, collecting digital images across the mounds. These images were collected to locate and identify the presence of possible chemosynthetic communities associated with the flux of methane through the seafloor, as well as to provide a characterization of the seafloor geology, to compare seafloor heterogeneity with seismic amplitude variations, and to identify locations of massive hydrate accumulations.

Survey Area

Occurrences of shallow and outcropping hydrate are common in the Gulf of Mexico (GOM), are found over a variety of water depths and constitute a dynamic environment changing on timescales of months to years (e.g., Brooks et al., 1994; Roberts and Carney, 1997). These mounds are typically associated with hydrocarbon seeps, gas charged sediments, and hardgrounds (Sager et al., 2003). Our cruise was run in the Mississippi Canyon in about 1300 m water depth, near lease block Atwater Valley 13, where two mounds have been identified as potential drilling targets for future JIP studies. Drilling will be funded by the Department of Energy in collaboration with the petroleum industry.

The area contains two features that appear as high relief mounds in high resolution seafloor bathymetric maps. They have been named mounds D and F. Mound F, in the southeastern regions of the survey area is the larger of the two mounds, standing at least 10 m above the background seafloor and with a diameter in excess of 200 m. Amplitudes of acoustic reflections from the seafloor on the mound are brighter than from adjacent seafloor, suggesting possible hard-bottom conditions associated with hydrate and/or authigenic carbonates. Deeper looking seismic reflection data show disturbances in the underlying seismic stratigraphy suggesting advection of gas and/or fluids from depths towards the mound. It has also been suggested that a shallow reflector beneath the mound represents a bottom simulating reflector (BSR) usually identified with the base of the hydrate stability zone or the top of a free (but trapped) gas layer. This suggests that hydrate might be stable within the mound and this prediction is apparently supported by proprietary cores containing hydrate that have been recovered from the mound

Mound D is also about 10 m in relief, but is smaller in diameter at less than 100m. It is also characterized by bright seafloor reflections. The disturbance to the deeper seismic stratigraphy is less beneath this mound suggesting lower fluxes to the seafloor.

In addition to the two mounds there are other patches of seafloor that are marked by bright seafloor acoustic returns and which might also represent hard-bottom conditions associated with hydrate and/or authigenic carbonates.

Equipment

EM System
The towed EM system we used was built at WHOI but is based on a design developed by colleagues at the Geological Survey of Canada. We have made some design changes to the original system, particularly to facilitate its operation in water depths from 1000-2500m. The system is dragged along the seafloor at speeds of 1-2 knots and makes measurements of seafloor resistivity approximately every 10m along track. The system has a CTD sensor mounted in the transmitter and so provides continuous measurements of bottom water salinity and temperature, important as the system traverses regions of fluid expulsion.

The raw data collected consist of 3 measurements of magnetic field amplitude and phase on each of three receivers. Data from each receiver are separately converted into apparent porosities by finding the best fitting equivalent half-space resistivity to the data and converting this value to porosity using an empirical relationship. The three apparent porosity values are essentially averages over different depths of seafloor. The closest receiver is 4m behind the transmitter and averages over about 2m of seafloor. The furthest receiver is 40m behind and provides information to a depth of about 20m. As the system is towed and measurements are made on each receiver, profiles of apparent porosity are built up.

Figure 1 A photograph of the towed EM system on deck. The system consists of a transmitter (large cylinder at right) connected to the ship by a 0.680 conducting cable. Three receivers (smaller cylinders) to behind the transmitter at separations of 4m, 13m and 40m and provide information to depths of about 20m subsurface.

Camera System
The WHOI Towed Digital Camera and Multi-Rock Coring System (TowCam) was developed to take advantage of advances in digital imaging technology and as been used for a wide range of seafloor science using both traditional, surface-ship methods, as well as nested surveys employing deep submergence vehicle systems.

The WHOI TowCam is an internally recording digital deep-sea camera system that also collects CTD water properties data. The TowCam is towed on a standard UNOLS 0.322" coaxial CTD sea cable, thereby permitting real-time acquisition of digital depth and altitude data that can be used to help quantify objects in the digital images. The system is shown on deck in Figure 2.

Navigation System
Primary navigation for G1-03-GM was by Differential Global Positioning System (DGPS), from a Communications System, Inc. (CSI) DGPS Max receiver that utilized wide area augmentation system (WAAS) corrections. YoNav software (developed by the USGS, version 3.14) logged the DGPS positions together with the gyro-compass heading and water depth, and provided a map display of position. A separate computer off the YoNav server provided a graphical monitor to assist bridge steering along tracklines. Features included in YoNav are cross-track distance off line, distance to go, distance along line, speed, and heading.
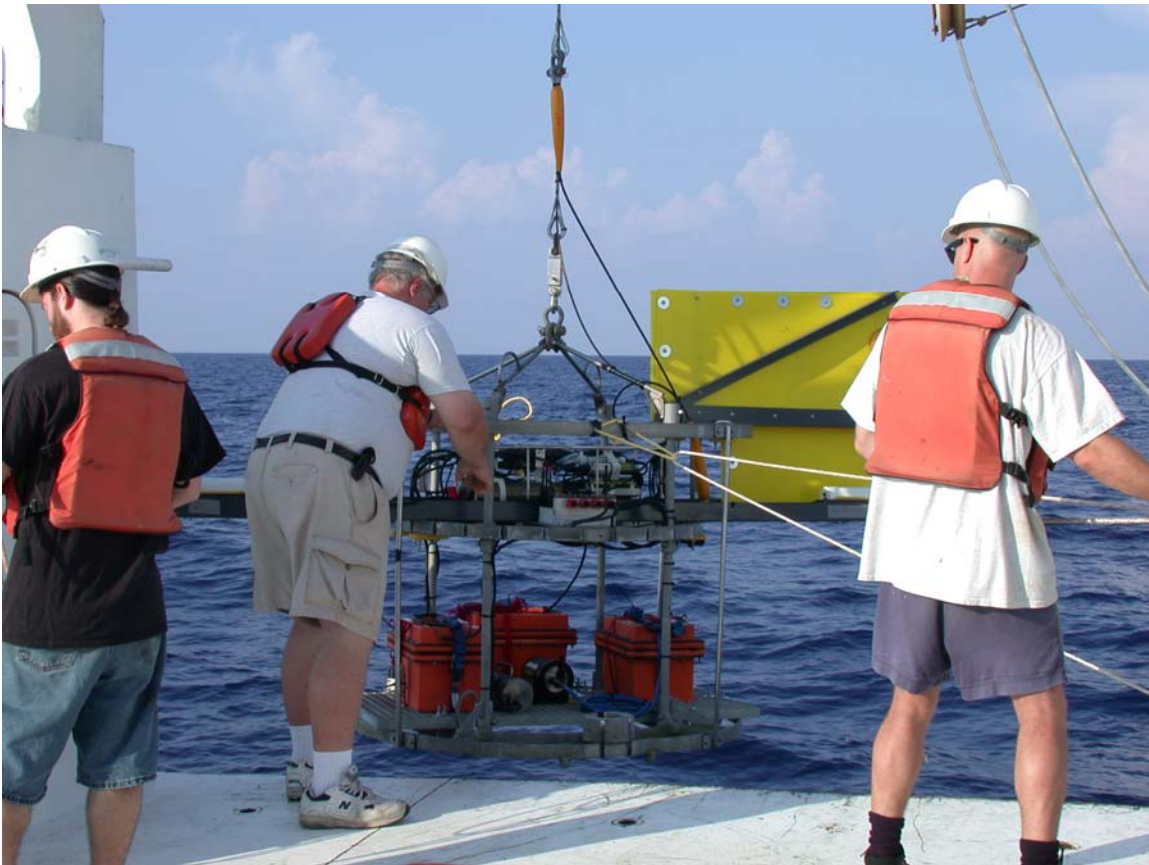

Figure 2. The WHOI TowCam being deployed from the Pelican. The system collects images of the seafloor with a digital camera housed in a pressure case towards the base of the system. The frame is flown at heights of between 3-5m above the seafloor. Height of the system is monitored by altimeters which telemeter their data up the coax CTD cable.

Summary of Coverage and Observations

The following descriptions of the data collected and of the observations made during the cruise are preliminary only and have not been rigorously checked at the level required for a peer-reviewed article. They serve as an overview and summary of cruise results. A full chronology of the ship operations is given in Appendix A.

Data Type	Line No	Coverage
Camera	1	531 Images
	2	1833 Images
	3	Aborted early
	4	1610 Images
	5	1999 Images
EM System	1	2.2 km of survey line
	2	2.2 km of survey line
	3	1.5 km of survey line
	4	2.1 km of survey line
	5	2.0 km of survey line
	6	2.0 km of survey line
	7	2.0 km of survey line
	8	0.8 km of survey line
	9	2.1 km of survey line

Table 1. A summary of the data coverage collected during the cruise.

During the cruise we completed one test run and three complete (longer than 6 hours) camera tows with excellent photographic results. Bottom visibility was generally excellent, and the camera sled could be towed 3-4 m above the seafloor yielding an image size of several square m (actual size is dependent on the altitude of the camera). About 6000 images were collected on transects across both mounds and on the seafloor between the mounds. Mussel communities are visible on the mounds, as well as crabs, worms, fish and other benthic animals (Figs 6, 7). The seafloor shows patchiness at the scale of the photographs, with dark blue/black areas, muddy brown areas, white areas, and occasional yellow tints being visible. Some of the boundaries between these regions are sharp (Fig. 6); others are gradational (Figs, 6,7). Photography taken after the EM tows also shows the track of the EM system across the muddy seafloor (cover image). Many of the tow tracks are non-linear (Figure 5) because of steering difficulties on the Pelican while maintaining the slow speeds required for the camera tows.

EM profiles were collected continuously for about 17 hours on 9 lines (Figure 4). Here we summarize some first order observations from the data. The EM data are presented as profiles of apparent porosities calculated from the best fitting half-space resistivity using the empirical Archie's law (Archie, 1942). In the past, we have found that such a presentation is the most intuitive way to display the raw data, especially in combination with coincident CTD conductivity and CTD depth profiles (Figure 8). Normally, there are three apparent porosity curves, one for each of the three receivers (as seen on Lines 1-3).

However, after line 3, the 4 m receiver failed and so for the remainder of the cruise we only recorded data on the 13 m and 40 m receivers.

EM data showed raised apparent porosities across both mounds and also at discrete locations on the surrounding seafloor. These raised porosities are in fact enhanced electrical conductivities which could be caused by (1) higher porosities, (2) raised sub-seafloor temperatures (3) raised chlorinities or (4) another conducting phase such as metallic sulphide mineralization within the seafloor. Since the apparent porosities in places are almost 100% (in some cases higher) we suggest that a combination of raised temperatures and pore water chlorinities are the most likely explanation. Across Mound F, the porosities increase (on the deepest looking 40 m receiver) from about 52 % to around 70 %. Assuming that the increase in conductivity is only due to an increase in temperature, this implies temperatures of about 30°C at depths of around 20 m below the seafloor. This seems higher than temperatures measured by heat-flow probes in the area (Wood et al., 2004 unpublished data), suggesting that chlorinity may also be a factor. The salinity needed to explain the increase in conductivity would be 65 compared to the background values of 35.6 (an increase of a factor of 1.8). Of course, these are upper-bound estimates as changes in both temperature and chlorinity could act together to raise bulk conductivity.

Figure 3. A map showing the location of Atwater Valley with respect to the coast of Louisiana. The track of the Pelican from its home port in Cocodrie, LA to the work site is also shown.
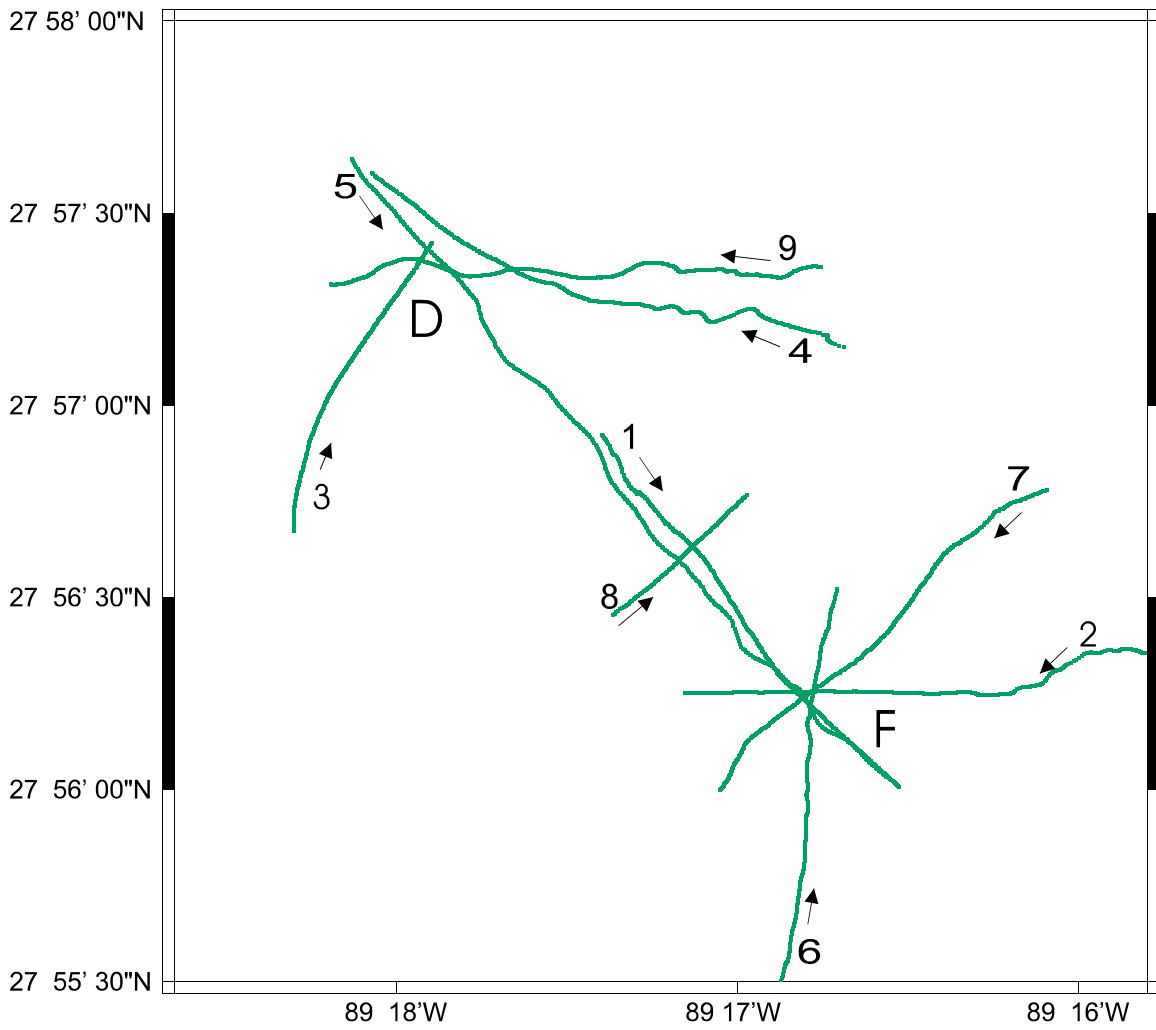
Figure 4. A map showing the lines completed with the EM system. The positions are uncorrected and are derived assuming a 700 m layback of the system from the ship. The lines converge on mounds D and F as shown.
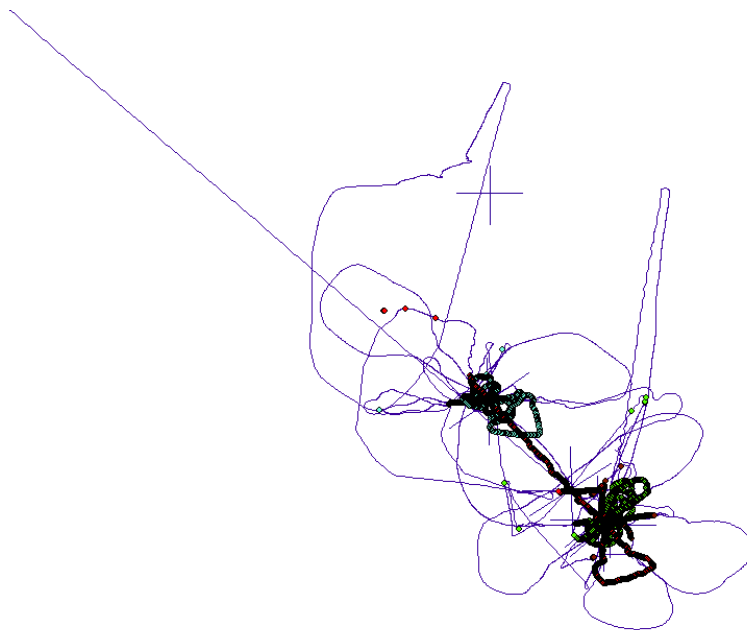
Figure 5. Ship tracks throughout the cruise. The camera tow coverage is highlighted by the dark symbols and is concentrated around the two mounds.
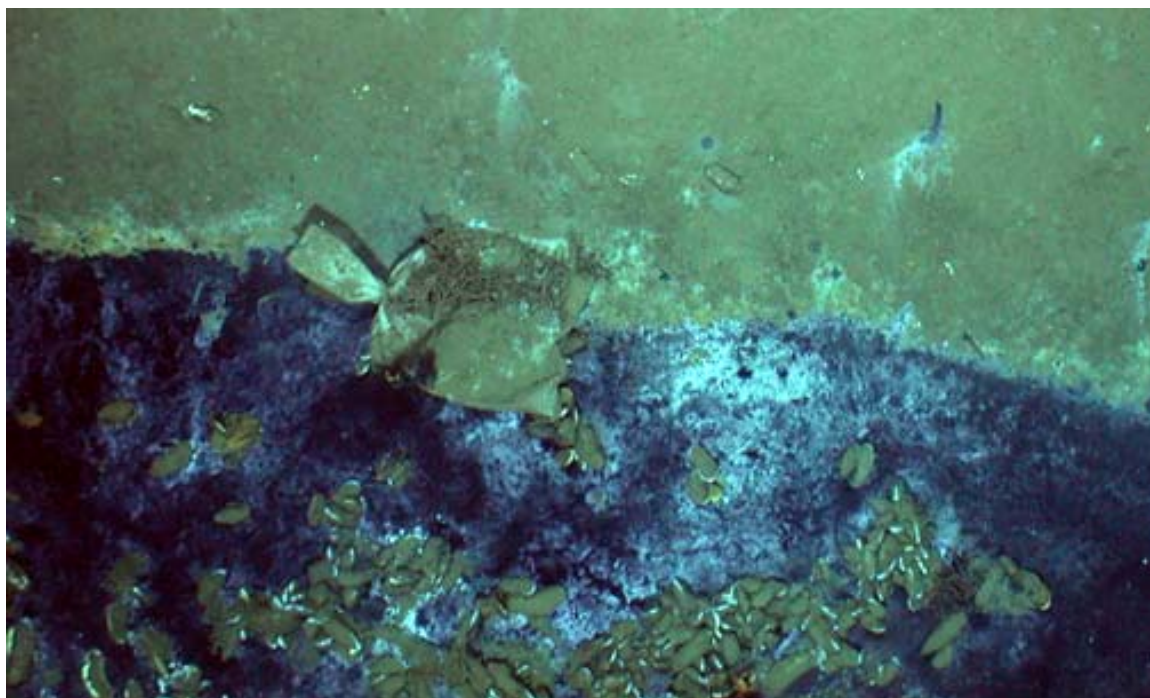

Figure 6. An example of a digital image of the seafloor collected on the northern mound (D) during the cruise. The image appears to show a food-sack deployed on the seafloor which appears to have been colonized by a variety of fauna. The transition from dark grey seafloor with patches of white to a brown muddy sediment was common across both mounds, but here it is sharply defined.
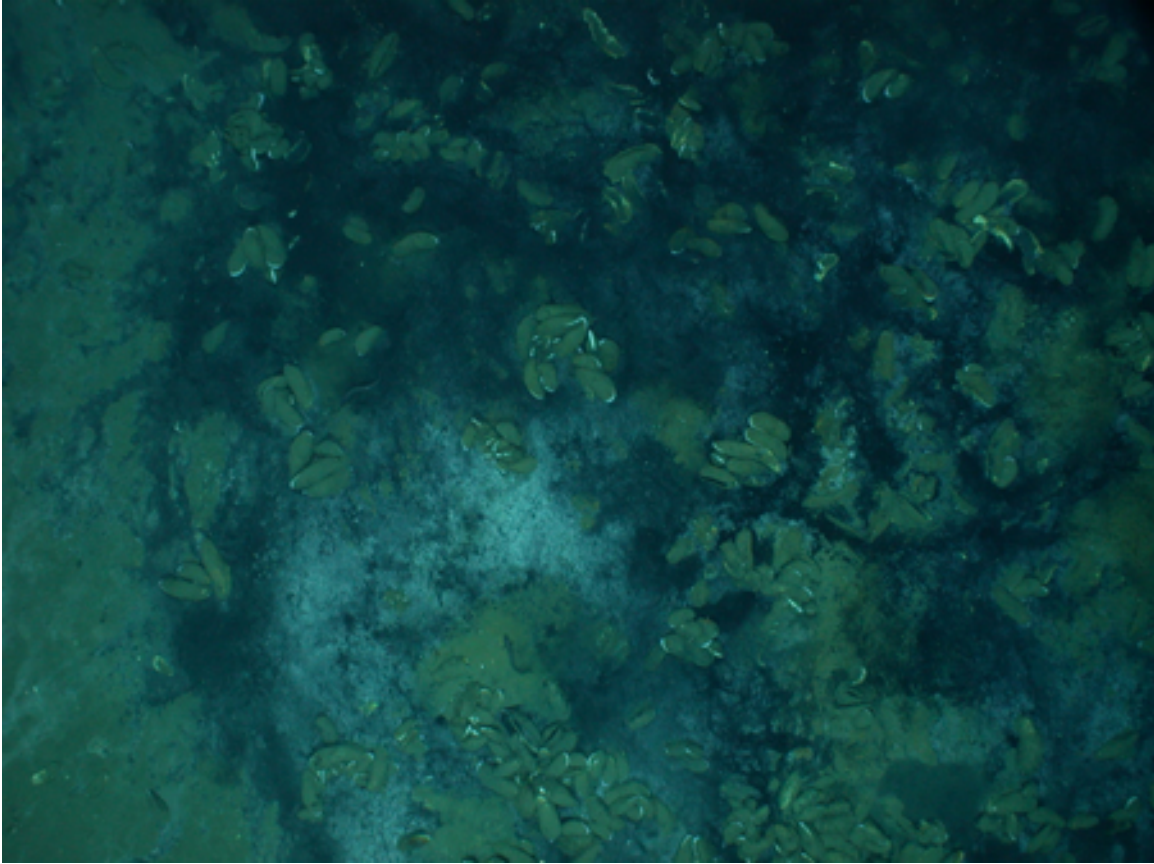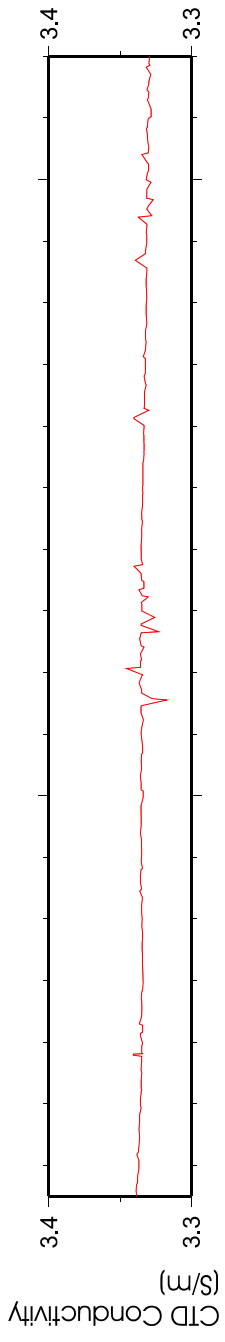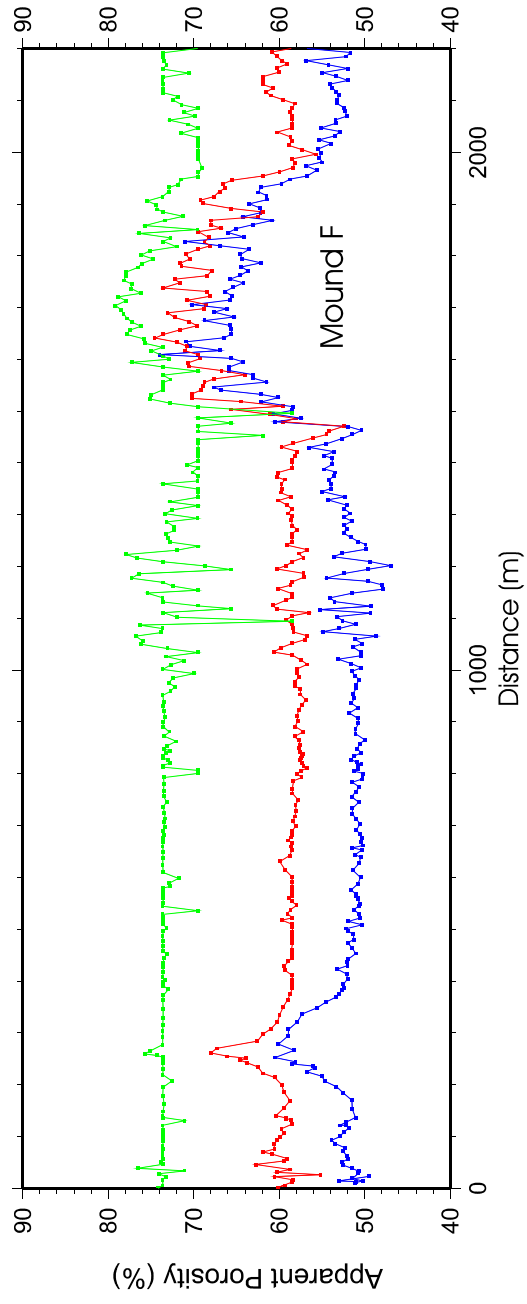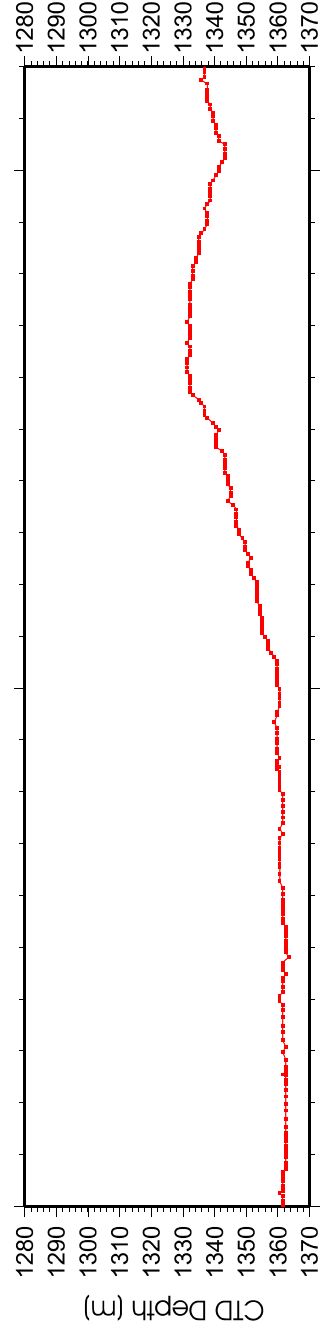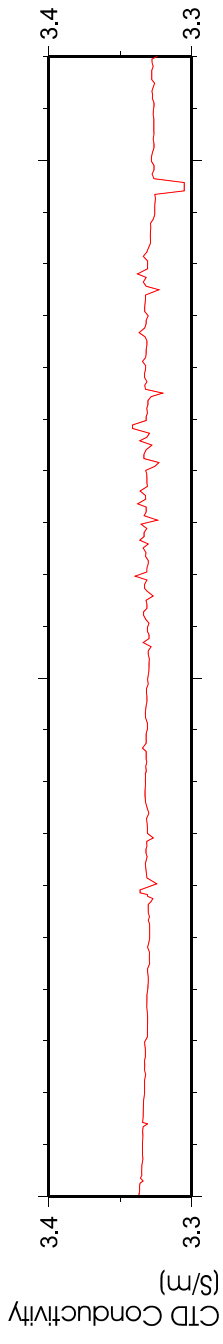
Figure 7 A digital image showing a mussel community on mound D. The boundaries between grey and white patches on the seafloor and the surroundings are less well defined here.

Figure 8. Below are examples of the EM data collected. The panels show (top) the conductivity measured by the CTD unit within the transmitter of the EM system (middle) the depth measured by the CTD unit (bottom) the apparent porosities measured by the system. The data are plotted as distance along track, relative to a starting position. On lines 1-3 we measured apparent porosities, one for each receiver. The data from the 4m receiver are shown in green. This receiver failed after the first three lines. The remaining lines only show data from the 13m (red) and 40m (blue) receivers.
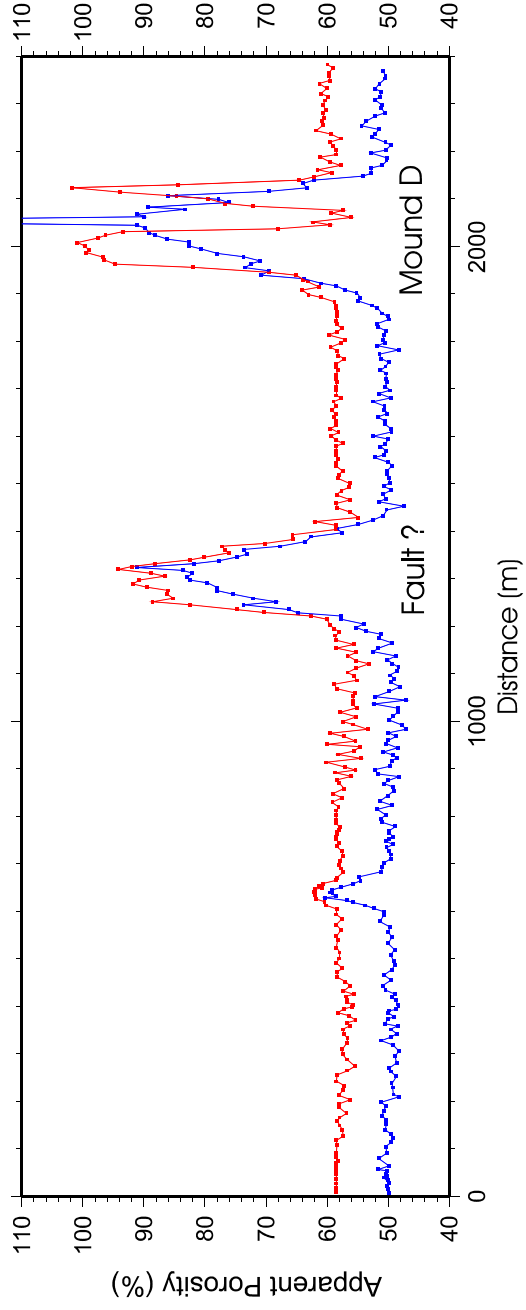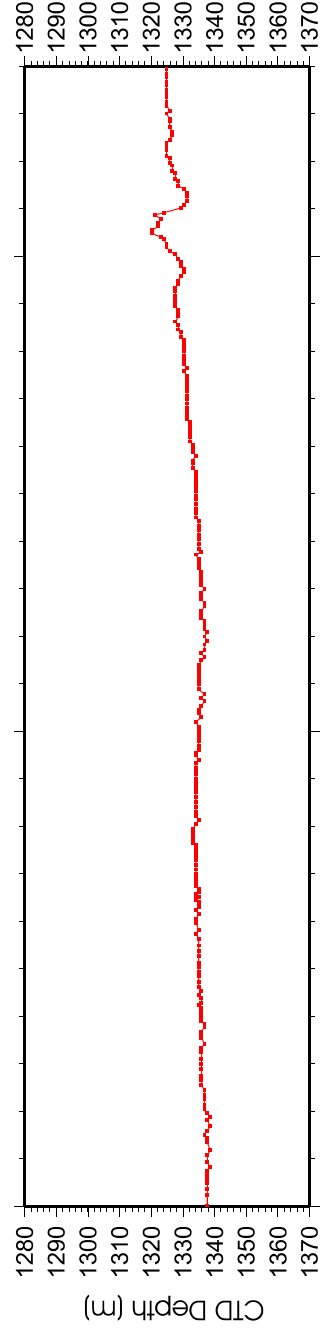
Line1

CTD Conductivity (S/m)

CTD Depth (m)

Apparent Porosity (%)

Distance (m)

Mound F

Fault ?

Line2

CTD Conductivity (S/m)

CTD Depth (m)

Apparent Porosity (%)

Mound F

Distance (m)

Line4

Line5

Mound D

Line8

CTD Conductivity (S/m)

CTD Depth (m)

Apparent Porosity (%)

Distance (m)

Seismic Bright Spot
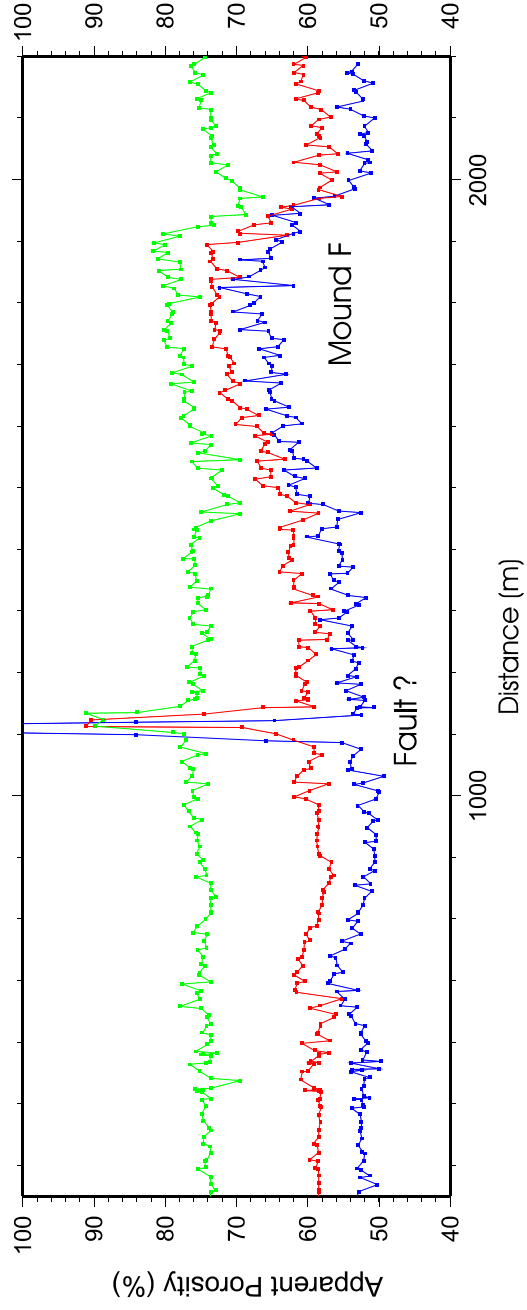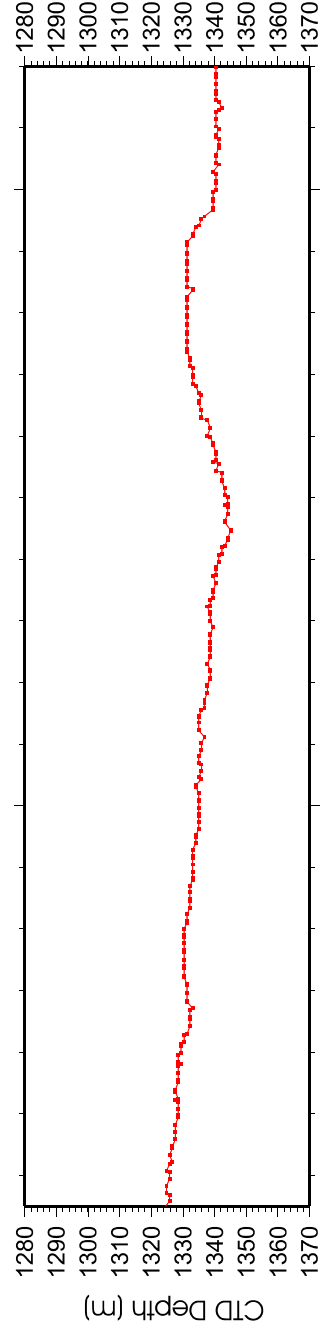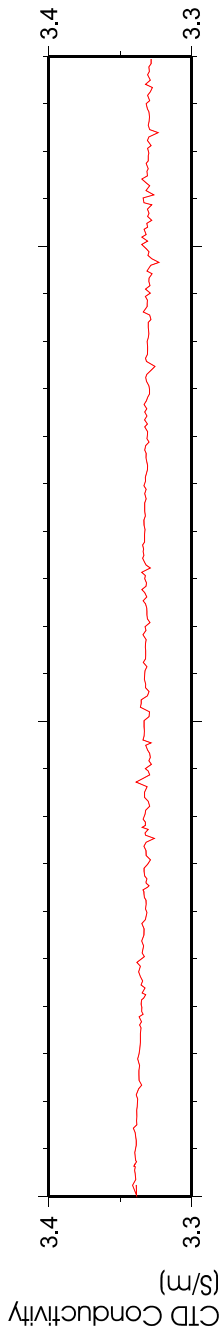
Summary

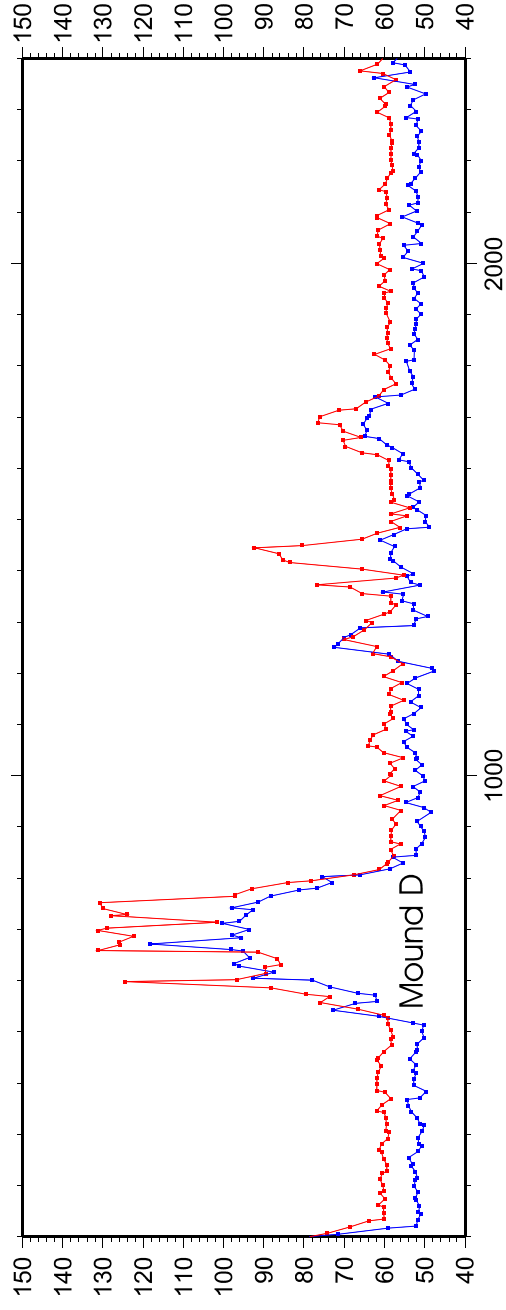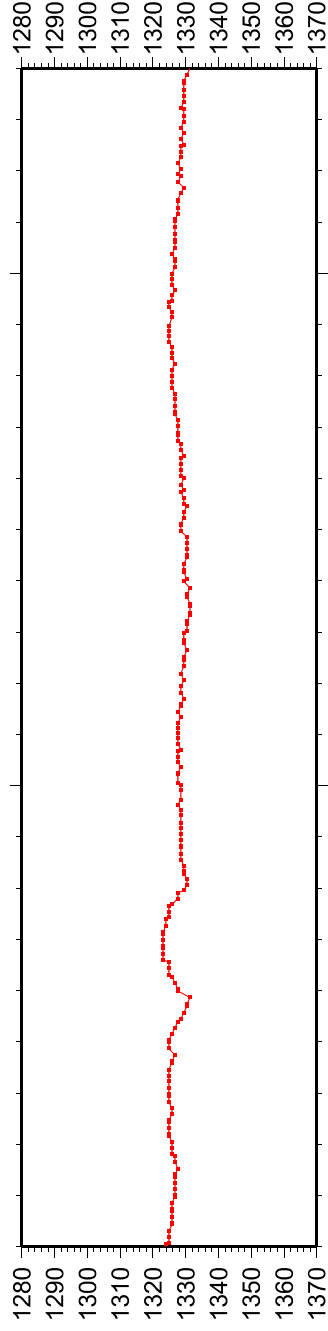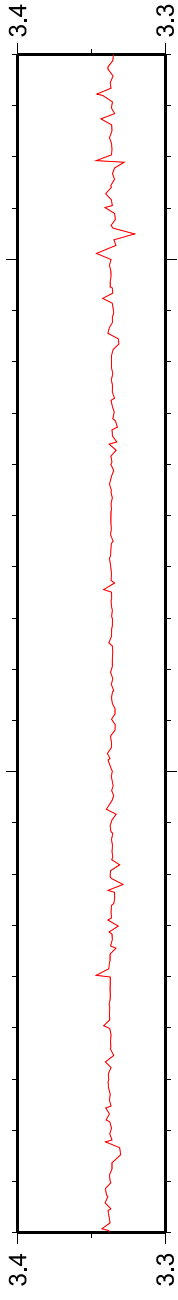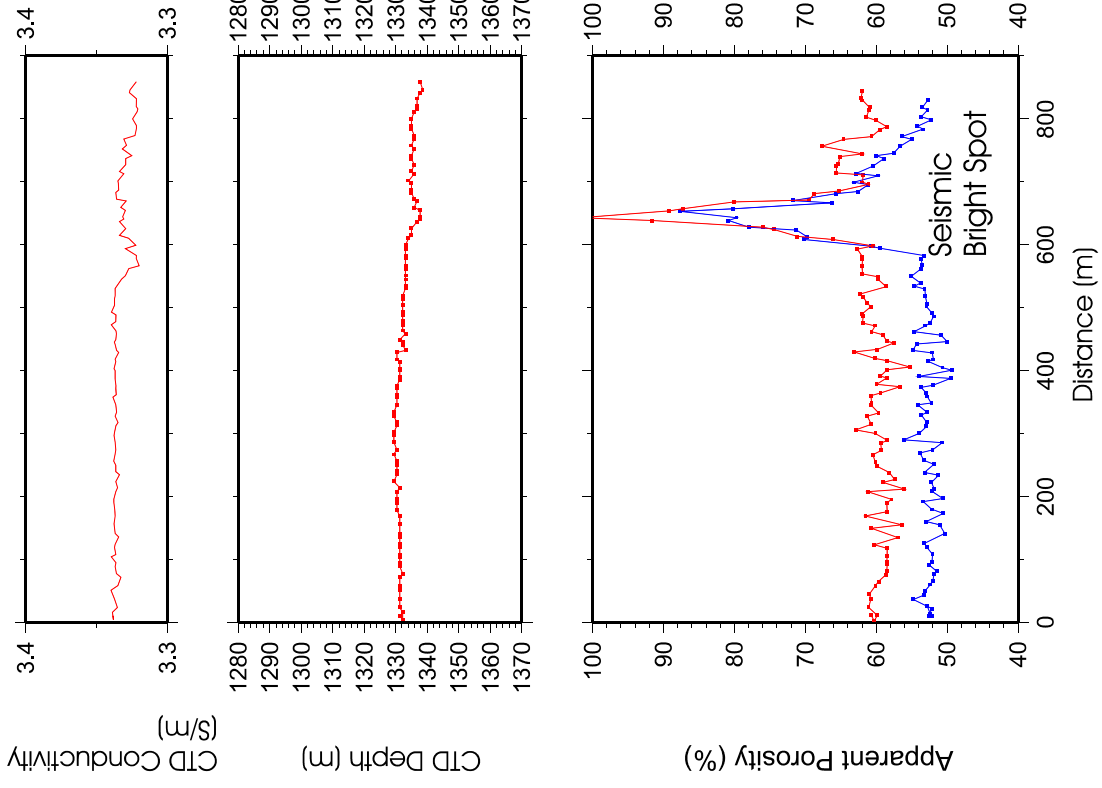The cruise was extremely successful, demonstrating for the first time that EM measurements respond to the internal structure of hydrate mounds. We collected nearly 17km of EM tow line. In addition, nearly 6000 digital images of the seafloor were collected which are in the process of being merged into a mosaic. Contrary to expectations, we saw no dips in apparent porosity suggesting the presence of massive hydrate and/or authigenic carbonates. Instead, the responses of the hydrate mounds as well as other locations in their vicinity were raised apparent porosities indicative of raised temperatures and/or pore water chlorinity in the subsurface. Based on the EM data and bottom photo-graphs we suggest that mound D, although smaller, appears the more active of the two mounds surveyed.

References

Archie, G.E., The electrical resistivity log as an aid in determining some reservoir characteristics. J. Pet. Technol., 5:1-8, 1942.

Brooks, J.M., M.C. Kennicutt, R.R. Fay, T.J. MacDonald and R. Sassen, Thermogenic gas hydrates in the Gulf of Mexico: Science, 223:696-698, 1984.

Evans, R.L., L. K. Law, B. St Louis, S. Cheesman and K. Sananikone, The Shallow Porosity Structure of the Continental Shelf of the Eel Shelf, Northern California: Results of a Towed Electromagnetic Survey, Marine Geology, 154, 211-226, 1999.

Hutchinson, D.R. and P.E Hart, Cruise report for G1-03-GM: USGS gas hydrates cruise, USGS open file report OF 03-474, 2004.

Kvenvolden, K.A., Gas Hydrates- Geological perspective and global change, Revs. of Geophys., 31:173-187, 1993.

Pearson, C. J. Murphy and R. Hermes, Acoustic and resistivity measurements on rock samples containing tetrahydrofuran hydrates laboratory analogues to natural gas hydrate deposits. J. Geophys. Res. 91:14,132-14,138, 1986.

Roberts, H.H., and R.S. Carney, 1997. Evidence of episodic fluid, gas and sediment venting on the northern Gulf of Mexico continental slope, Econ. Geol., 92:863-879.

Sager, W.W, MacDonald, I.R. and Hou, R., Geophysical signature of mud mounds at hydrocarbon seeps on the Louisiana continental skope, northern Gulf of Mexico, Marine Geology, 198, 97-132, 2003.

Sloan, E.D., Clathrate hydrates of natural gases, Marcel-Dekker, New York, 714pp, 1998.

Appendix A: Chronology
Times below are in UTC, except where stated.
June 20th (172)
Depart LUMCON approx 18:00 local time
June 21, 2004 (173)
Arrive on station approx 0700 hrs local
12:55 Deploy camera system for short test run over mound F. The camera system was run on the CTD cable. The CTD winch had been turned prior to the cruise to provide a clear path over the stern. The wire was run through a block offset to starboard in the Stern A-frame.
13:22 First picture taken. For most of this test deployment the camera was directly beneath the ship. Ship handling with the camera above bottom was difficult as the camera ideally needs to be towed at speeds less than about ½ knot. Height of the camera was controlled in the winch dog-house with altitudes provided by an altimeter on the camera frame. A series of images were taken at different heights across the hydrate mound to ascertain the ideal height for surveying.
14:16 End of tow.
14:47 Recover camera and download pictures. Images at 3-4m are good and show patchy areas of grey and white across mound, possibly hydrate and carbonate.
16:10 Re-deploy camera for full tow.
16:37:30 First picture taken. Layback on this tow varied from about 300m to 700m. Lines completed: 1, 6 and 11.
22:00 end of line 11. Camera recovered.
June 22nd (174)
00:55 EM system deployed and switched on.
01:23   System on bottom, but kiting a little. First line more or less co-incident with seismic line 65, although no crossing of mound D.
02:35 End of line 1.
03:12 Start of line 2 (seismic line 97).
04:11 End of line 2
04:12 line 2b – transit line to north.
04:27 End line 2b.
04:52 Start of line 3 (seismic line 75). Difficulty with ship handling meant that we could not closely follow line 75.
05:42 End of line 3. Lose 4m receiver just before end of line. Receiver will be intermittent (works in water column) for rest if cruise before dying completely.
In water column: 4m receiver shows 102% porosity; 13m 100% and 40m 110% (but oscillating).
06:28 Start of line 4 (Seismic line 94 across mound D). See several positive porosity anomalies along this line including one as we cross the mound.
07:50 end of line 4.
9:17 Start of line 5 – rerun of seismic line 65, this time attempting to cross mound D. Problems with depth control at end of line.
11:05 End of line 5.

11:32 Start of line 6.
12:25 End of line 6.
13:03 Start of line 7 (Seismic line 82)
14:23 End of line 7.
15:18 Start of line 8
15:47 End of line 8
16:24 Start of line 9
17:50 End of line 9.
18:05 Start calibration
19:20 Start array recovery.
21:11 Start camera tow 3.
21:41:35 First picture.
22:09 End tow 3. Trouble with one of the altimeters. Recover camera to make setting adjustment.
23:15 Start camera tow 4.
23:45 First picture. Lines completed USGS lines 13, 12, 5, 13, 12, 1.
June 23rd (175)
04:25 End tow 4.
13:15 Start tow 5. Camera in the water
13:43:55 First picture. Lines completed USGS lines 2, 6, 14, 4, 6, 2, 8, 2, 10.
19:17 End of Line. Recover camera.
20:00 (approx) depart work area for LUMCON.